The Human Visual Pathway Communicates Directly With the Subarachnoid Space

Henrik Holvin Jacobsen,[1,2] Geir Ringstad,[3] Øystein Kalsnes Jørstad,[1,2] Morten C. Moe,[1,2] Tiril Sandell,[1] and Per Kristian Eide[2,4]

[1]Department of Ophthalmology, Oslo University Hospital, Oslo, Norway
[2]Institute of Clinical Medicine, Faculty of Medicine, University of Oslo, Oslo, Norway
[3]Division of Radiology and Nuclear Medicine, Department of Radiology, Oslo University Hospital, Rikshospitalet, Oslo, Norway
[4]Department of Neurosurgery, Oslo University Hospital, Rikshospitalet, Oslo, Norway

PURPOSE. Explore in vivo whether there is direct communication between the cerebrospinal fluid (CSF) and extravascular compartment of human visual pathway structures.

METHODS. A prospective and observational study included 10 subjects who underwent intrathecal gadolinium–enhanced magnetic resonance imaging (MRI) for suspected CSF circulation disorder, but with a negative result and with no known ophthalmic diseases. After precontrast T1-weighted MRI, 0.5 mL of gadobutrol (Gadovist, 1.0 mmol/mL) was injected intrathecally. Gadobutrol distributes in the extravascular space, and served as a CSF tracer. Consecutive MRI scans were obtained throughout 24 to 48 hours. To assess gadobutrol contrast enrichment, regions of interest (ROIs) were placed at multiple locations along the visual pathway, from the primary visual cortex to the eye's vitreous body. CSF tracer dependent T1 signal was measured in each ROI. A linear mixed-model was used for statistical analyses.

RESULTS. CSF tracer enrichment was found within the optic nerve, optic chiasm, optic tract, and primary visual cortex ($P < 0.001$). Peak tracer enrichment in the visual pathway generally occurred after 24 hours and was preceded by peak enhancement in the prechiasmatic cistern after 4 to 6 hours.

CONCLUSIONS. The results indicate direct communication between CSF of subarachnoid space and the extravascular space of the human visual pathway. Extravascular entry of the CSF tracer is a prerequisite for a glymphatic system, the present findings may suggest its presence. The existence of a glymphatic system in the human visual pathway could bring novel perspectives on the pathophysiology and treatment of ophthalmic diseases.

Keywords: glymphatic circulation, visual pathways, magnetic resonance imaging, optic nerve, cerebrospinal fluid

Since the first report in 2012 of a glymphatic system within the central nervous system (CNS), evidence has accumulated for the existence of this paravascular route for transport of solutes in the brain.[1–4] According to the concept, cerebrospinal fluid (CSF) of the subarachnoid space (SAS) communicates directly with interstitial fluid of the brain parenchyma, enabling for convective CSF flux to clear the brain of potentially toxic metabolites.[4,5] The glymphatic system is also suggested to be a carrier of solutes from CSF to the entire brain parenchyma.[6] Although the glymphatic system has mostly been studied in animals, recent evidence suggests a corresponding human glymphatic system.[1,6,7] The existence of a glymphatic system within the human visual pathway, however, remains an unresolved issue; yet, limited data have indicated this.[8–15]

The aim of this study was to examine whether a CSF tracer, gadobutrol (Gadovist; Bayer Pharma AG, Berlin, Germany) administered intrathecally distributes in the extravascular space within the orbital and intracranial segments of the optic nerve and the central visual pathway. Evidence of such tracer distribution would indicate a direct communication between the CSF and the extravascular space of the visual pathway, suggesting a paravascular inflow route (i.e., a prerequisite for a glymphatic system). Its existence in the human visual pathway could implicate a novel view on ophthalmic pathophysiology and treatment strategies.

MATERIALS AND METHODS

Approvals

Study approval was granted by the institutional review board of Oslo University Hospital (2015/1868), The Regional Committee for Medical and Health Research Ethics of Health Region South-East, Norway (2015/96), and the Norwegian Medicines Agency, Norway (15/04932-7). Inclusion was by written and oral informed consent after explaining the nature and the possible consequences of the study. The study was conducted in compliance with the tenets of the Declaration of Helsinki.

Experimental Design and Study Population

From an ongoing prospective study cohort of 100 subjects, all individuals ($n = 10$) without intrathecal contrast–enhanced magnetic resonance imaging (MRI) evidence of disrupted CSF

TABLE 1. Patients

N	10
Age, y, mean (SD)	36.9 (± 6.95)
Sex, female/male	8/2
BMI, kg/m², mean (SD)	27.2 (± 5.15)
Comorbidity	
Hypertension	0
Diabetes	1
Indication for MRI	
Spontaneous intracranial hypotension	3
Pineal Cyst	7

BMI, body mass index.

flow were included in the present study. The subjects were (1) patients with clinical suspicion of CSF leakage in whom no CSF leakage was found ($n = 3$), and (2) patients in whom a pineal gland cyst was considered an incidental finding and managed conservatively ($n = 7$). None of the subjects had previously been examined with gadobutrol. For the three patients with clinical suspicion of CSF leakage, one had previously been treated for a meningocele, one had formerly undergone a lumbar puncture that was followed by chronic headache, and one had headache, tinnitus, and conventional MRI suspicion of intracranial hypotension. For the patients with a pineal gland cyst, headache (7/7), nausea (6/7), fatigue (4/7), and cognitive deficit (4/7) were the main complaints leading to MRI work up. No other neurosurgical procedures had been performed in the cohort. None of the subjects had known ophthalmic disease or complaints registered at admission; therefore, they were not seen by an ophthalmologist as part of the clinical work-up. The patient demographics are presented in Table 1. All individuals were managed at the Department of Neurosurgery, Oslo University Hospital, Rikshospitalet, Oslo, Norway. None of the data used in the current study have been previously published.

Study participants underwent MRI before and at multiple time points after intrathecal lumbar administration of the MRI contrast agent gadobutrol (0.5 mL of 1 mmol/mL; Gadovist) used as CSF tracer. The study subjects were examined in the period from February 2016 to August 2018. Exclusion criteria were as follows: history of hypersensitivity reactions to contrast agents, history of severe allergy reactions in general, evidence of renal dysfunction, pregnant or breastfeeding women, and age under 18 or older than 80 years.

MRI Protocol

For a more detailed description, please refer to a previous article.[7] In brief, we obtained three-dimensional (3D) T1-weighted volume scans using a 3 Tesla Philips Ingenia MRI scanner (Philips Medical Systems, Best, the Netherlands). The imaging protocol settings were identical at all time points. A total of 184 overlapping slices were reconstructed to 368 slices, each 1-mm thick.[7]

Intrathecal Administration of Gadobutrol

Following precontrast MRI, 0.5 mL of 1.0 mmol/mL gadobutrol was injected intrathecally by X-ray–guided lumbar puncture performed by an interventional neuroradiologist. There are no gadolinium-based MRI contrast agents approved for intrathecal use; therefore, gadobutrol was used with special permission granted from the Norwegian National Medicine Agency. Furthermore, this study included an intrathecal injection procedure, which, due to ethical considerations, is not performed in healthy individuals. There were no serious

adverse events to gadobutrol administration. A more comprehensive description can be found in Ringstad et al.[7]

Postcontrast MRI Acquisitions

Following gadobutrol administration identical and consecutive MRI examinations were performed at the following time points: 0 to 20 minutes; 20 to 40 minutes; 40 to 60 minutes; 1 to 2 hours; 2 to 4 hours; 4 to 6 hours; 6 to 9 hours; 24 hours (48 hours in 5 subjects). The subjects remained in a supine position throughout the 6- to 9-hour scan and were then allowed to move without restrictions.

Image Analysis

The MRI volume scans were postprocessed with multiplanar reconstructions in the oblique coronal plane perpendicular to the long axis of the optic nerve and optic tract using the radiology software Sectra Picture Archiving and Communication System (PACS; IDS7; Sectra AB, Linkoping, Sweden). The optic chiasm and primary visual cortex regions of interest (ROIs) were placed on standard coronal and axial sections, respectively. For each time point ROIs were placed along the visual pathway structures (Fig. 1). Except for the chiasm, the ROIs were placed bilaterally and symmetrically in the mentioned visual pathway structures. As neither the lateral geniculate body nor the superior colliculus could be properly segmented on the T1-weighted scans, these structures were not included. Each ROI provides a mean of signal units at the image grayscale. Signal units can be compared between time points and study subjects after normalization to a reference level. The superior sagittal sinus was used as reference.[7] The ROIs were placed in the centre of the tissue of interest to avoid partial volume averaging defects. The ROIs were positioned by the first author (HHJ), and correct placement was verified by a neuroradiologist (GR). The following ROIs were used: the vitreous body, three separate sections of the intraorbital segment of the optic nerve (retrobulbar, middle, and posterior part), prechiasmatic segment, CSF near optic chiasm, optic chiasm, optic tract, and a ROI representing primary visual cortex. All bilateral measurements were averaged. The placement of ROIs is shown in Supplemental Figures S1 and S2.

Statistics

Continuous data were described as mean with standard deviation or mean with standard error. Repeated measurements were assessed with linear mixed-models using a random intercept, robust standard error, and maximum likelihood estimation. For the statistical analyses we used SPSS version 22 (IBM Corporation, Armonk, NY, USA) or Stata/SE version 15.0 (StataCorp LLX, College Station, TX, USA). Statistical significance was accepted at the 0.05 level.

RESULTS

Following intrathecal administration of gadobutrol, serving as a CSF tracer, a rapid signal increase due to tracer enrichment occurred within the CSF of the prechiasmatic cistern (Fig. 2). The trend plot shows peak enhancement after 4 to 6 hours; at group level, the normalized signal units increased by 3826% (±1958) compared with precontrast images (Table 2). Accordingly, there was a strong enhancement of CSF tracer within the CSF of the prechiasmatic cistern.

There was a highly significant CSF tracer enrichment within all three intraorbital optic nerve segments (Figs. 3b–d). Peak enrichment occurred after 24 hours (Fig. 3), with an average
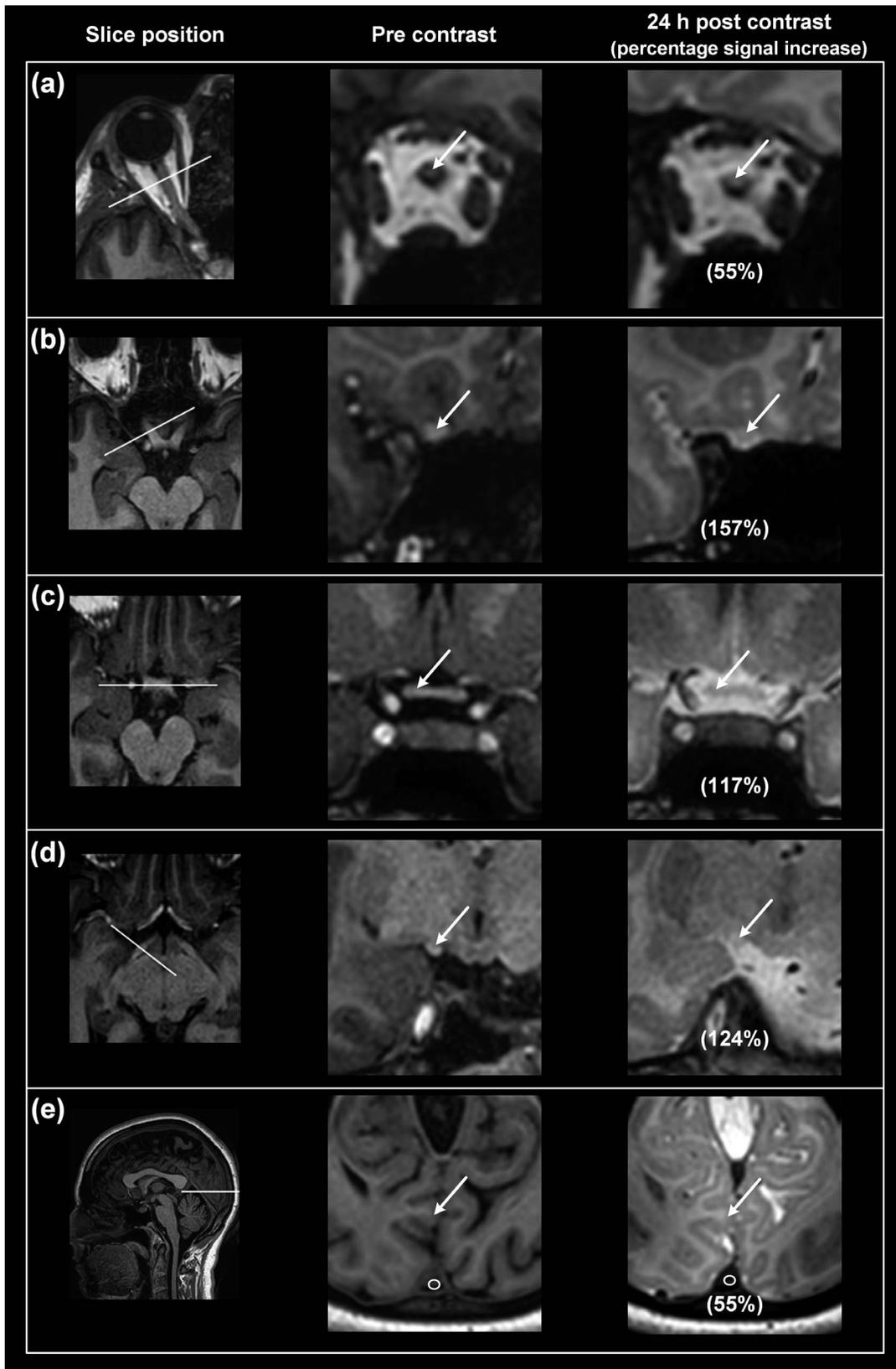
FIGURE 1. T1-weighed MRI: slice sections and measurement areas. Images in the *left column* demonstrates slice sections with corresponding images in the same row. *Arrows* (and the *circle* in superior sagittal sinus [SSS]) indicate positioning of ROIs, which are left out from the illustration to allow direct inspection of the anatomical structures and their contrast enhancement. A typical circular ROI is, however, exemplified in figure element (**e**). The *middle* and the *right column* show magnified images obtained before intrathecal injection with gadobutrol (Gadovist) and 24 hours postinjection, respectively. The letters (**a–e**) in the *left column* correspond to the following structures: optic nerve (*middle part*) (**a**); prechiasmatic segment of the optic nerve (**b**); optic chiasma (**c**); optic tract (**d**); and primary visual cortex and SSS (**e**). A change in T1 signal from baseline to the peak at 24 hours is clearly seen in all the structures.
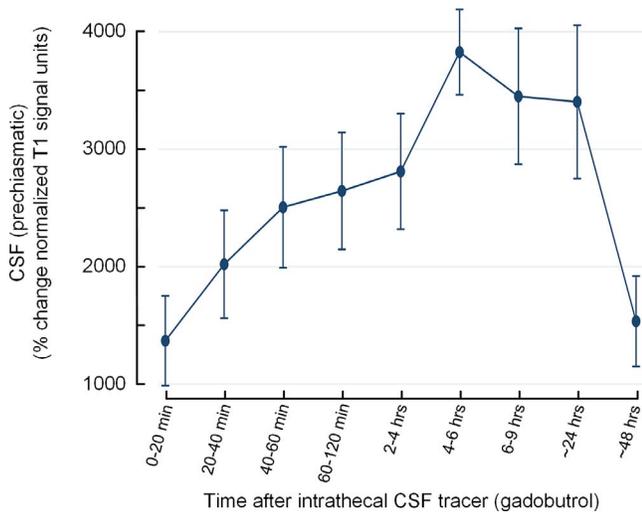
FIGURE 2. Enhancement of CSF tracer within the prechiasmatic cistern. Trend plot of percentage change in signal unit ratio within the CSF of the prechiasmatic cistern ($P < 0.001$). The trend plot is presented with mean (points) ± standard error (SE) (*bars*).

signal increase of 136% (±119; retrobulbar part), 95% (±72; middle part), and 78% (±64; posterior part) (Table 2).

The time-dependent CSF tracer enhancement within the intracranial visual pathways is presented in Figure 4. There was a highly significant enrichment of CSF tracer within the prechiasmatic optic nerve (Fig. 4a), optic chiasm (Fig. 4b), optic tract (Fig. 4c), and gray matter of the primary visual cortex (Fig. 4d). Within these structures peak CSF tracer enrichment occurred after 24 hours, except for the optic chiasm, in which a peak was seen after 6 to 9 hours. The negative values in some of the time points (Figs. 3, 4; Table 2) are likely due to measurement inaccuracies, because a true decline in T1 signal should not be expected. The average signal increase after 24 hours was 110% (±78; prechiasmatic part of optic nerve), 74% (±64; optic chiasm), 101% (±91; optic tract), and 67% (±50; primary visual cortex).

There was no evidence of gadobutrol enhancement in the central venous space (data not shown).

The percentage signal increase for the various ROIs is summarized in Table 2. There was a significant signal increase ($P < 0.001$) in all regions over time, except for the vitreous

body, in which only a nonsignificant positive trend was evident (Fig. 3a).

DISCUSSION

The main result of the present study was a highly significant enrichment of a CSF tracer within the visual pathways. This in vivo finding may indicate that the recently described brain glymphatic system also extends to the visual structures in humans. Glymphatic circulation as a concept was introduced by Nedergaard and colleagues[4] in 2012 and refers to a cerebral, paravascular route for transport of solutes. Based on rodent studies it was suggested that CSF of the subarachnoid space is in direct communication with the brain's interstitial fluid via a paravascular, aquaporin-4 channel (AQP4)-dependent route. It was further proposed that the glymphatic system provided a clearance route for waste products of cerebral metabolism. Subsequently, evidence was given that the function of the glymphatic system is highly dependent on sleep and is impaired with age.[16,17] The first evidence of a human glymphatic system was provided in 2015.[18] In vivo studies have shown that human glymphatic functions generally differ from animals.[1,6,7] For instance, human studies have shown brain-wide enrichment of a CSF tracer, whereas animal studies have presented evidence for glymphatic circulation as a primarily cortical phenomenon. Moreover, whereas the glymphatic circulation occurs rapidly in animals (peak cerebral CSF tracer enrichment after 1–2 hours), it takes place as a protracted phenomenon in humans (peak cerebral CSF tracer enrichment after 24 hours). A possible contributing factor to the much faster peak in animals could be the smaller distances in the rodent's brain. We had no measurements between the 6- and 9-hour scan and the next morning, thus we cannot with certainty claim that the true peak was at 24 hours.

The first publications proposing an ocular glymphatic system that extends to the optic nerve and retina were published in 2015.[10,15] Early hypothesis-driven reports were based on extrapolation of findings from rodents brains, but subsequent papers added to the evidence for a human ocular glymphatic system[8,9,11,12] In a postmortem study of the human optic nerve, carried out by Wostyn et al.,[12] India ink was shown to accumulate in the nerve's paravascular spaces while leaving the vascular lumen unlabeled. Moreover, after injecting fluorescent dextran into the cisterna magna of mice, Mathieu et al.[13] observed dextran within the optic nerve. The CSF tracer entered the optic nerve along paravascular routes, which were ensheathed with aquaporin-labeled astrocytic

TABLE 2. Percentage Change in Signal Unit Ratio at Some Time Points After Intrathecal Gadobutrol

| Anatomic Region | Time After Intrathecal Gadobutrol | | | | | | Significance |
	1–2 h	2–4 h	4–6 h	6–9 h	24 h	48 h	
CSF							
CSF (prechiasmatic cistern)	2644 ± 1492	2810 ± 116	3826 ± 1088	3449 ± 1828	3403 ± 1958	1535 ± 1086	<0.001
Orbital compartment							
Vitreous body	7 ± 29	9 ± 26	12 ± 31	11 ± 26	22 ± 42	19 ± 27	0.24
Optic nerve (retrobulbar)	1 ± 24	29 ± 74	41 ± 80	96 ± 105	136 ± 119	133 ± 76	<0.001
Optic nerve (mid)	−2 ± 19	6 ± 24	19 ± 14	52 ± 59	95 ± 72	84 ± 42	<0.001
Optic nerve (posterior)	−1 ± 29	−6 ± 27	32 ± 38	63 ± 55	78 ± 64	52 ± 49	<0.001
Intracranial compartment							
Optic nerve (prechiasmatic)	4 ± 16	32 ± 29	67 ± 40	99 ± 76	110 ± 78	59 ± 41	<0.001
Optic chiasm	6 ± 28	23 ± 35	60 ± 48	76 ± 38	74 ± 64	32 ± 23	<0.001
Optic tract	5 ± 19	23 ± 21	63 ± 50	85 ± 67	101 ± 91	43 ± 41	<0.001
Primary visual cortex (gray matter)	−4 ± 11	2 ± 15	7 ± 24	27 ± 25	67 ± 50	59 ± 70	<0.001

Percentage signal change given as mean ± SD. Statistical differences determined by a linear mixed-model for repeated measurements.
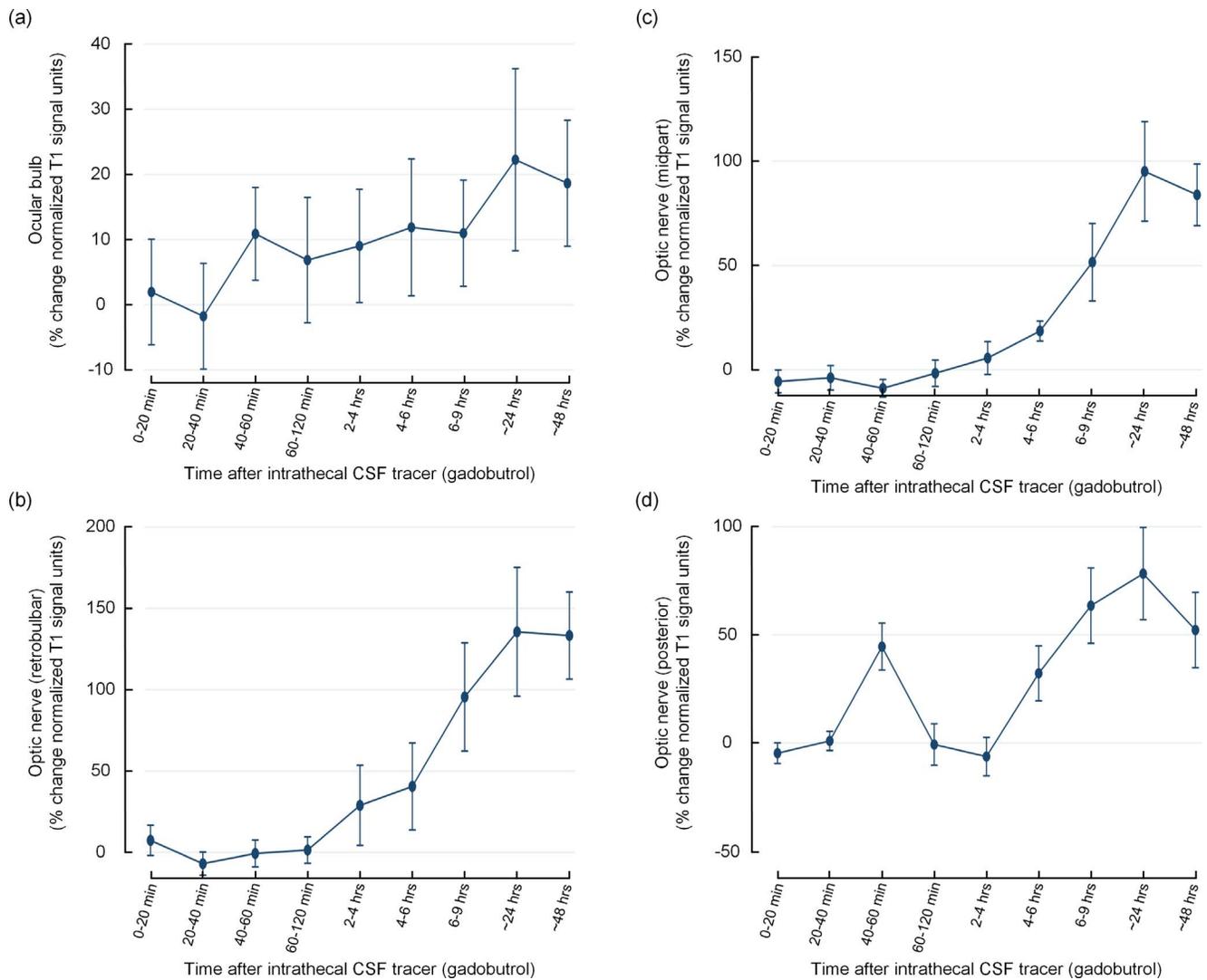
FIGURE 3. Enhancement of CSF tracer within the orbital visual pathways. Trend plots of percentage change in signal unit ratio are shown for (a) ocular bulb (vitreous body; $P = 0.24$), (b) optic nerve (retrobulbar; $P < 0.001$), (c) optic nerve (midpart; $P < 0.001$), and (d) optic nerve (posterior, $P < 0.001$). Trend plots are presented with mean ± SE.

endfeet. As the measurements were done at a single time point, the study did not assess the tracer dynamics.

The paravascular space is ensheathed by astrocytic end-foot processes, which are separated with small inter-end-feet gaps.[19] The astrocytic end foot processes are covered with AQP4 channels, which facilitate transport of water between the paravascular compartment and the interstitial space.[19] These AQP4 channels have a small diameter of approximately 1.5 Å (1 Å = 0.1 nm).[20] The inter-end-feet gaps may allow for molecules of up to 20 nm in diameter to pass through.[19] Dextran, with a known hydrodynamic diameter of 2.6 nm, has molecular weight of 3000 Da and is thus comparable to gadobutrol with molecular weight of 604 Da.[6] AQP4 channels are presumably too narrow for gadobutrol to cross. Instead, we suggest the inter-end-feet gaps facilitate entry of gadobutrol from the paravascular into the interstitial space. It has been hypothesized that loss of perivascular AQP4 could lead to impaired glymphatic flow.[4] Signs of impaired glymphatic clearance function has been found in patients with idiopathic normal pressure hydrocephalus,[6,7] for which perivascular AQP4 expression is reduced.[21,22]

Because the MRI resolution is limited to 1 mm, we cannot determine the paths taken by the CSF tracer, gadobutrol, at a microscopic level. Also, as visual pathway structures lie in close proximity to the CSF, effects of molecular diffusion behind visual pathway enrichment cannot be ruled out. However, as gadobutrol does not cross the intact blood–brain barrier (BBB),[23] it can be deduced that the tracer is confined to the extravascular space. In the work by Mathieu et al.,[13] tracers of different sizes were used, Dextran-10 being the smallest. The tracers were observed to enter the optic nerve via paravascular spaces and not by diffusion from the perioptic SAS. Diffusion over the glia limitans would be expected to occur through astrocytic intercellular clefts (20 nm).[19] Dextran-10 has a calculated diameter of 4.6 nm.[24] Although dextran-10 is a much bigger molecule than gadobutrol, they are comparable in this context. Based on a growing body of experimental evidence[4,5,13,14,25] and the known properties of gadobutrol, a plausible explanation to the present observations is that gadobutrol, equivalent to the rodent studies by Mathieu et al.,[13] entered the optic pathway through paravascular spaces. Moreover, we consider it likely that the tracer enrichment was due to influx of gadobutrol into the interstitial space. We
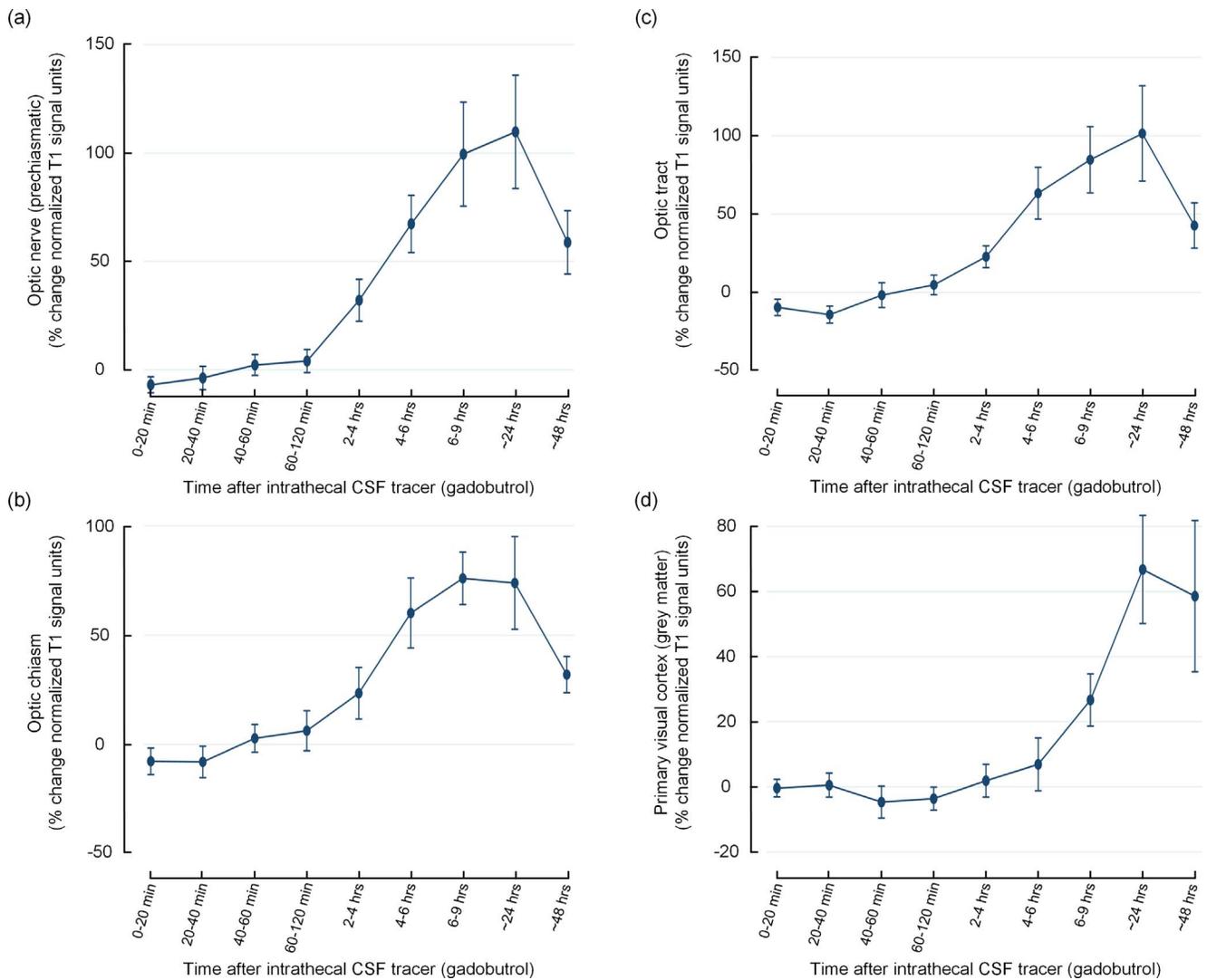
FIGURE 4. Enhancement of CSF tracer within the intracranial visual pathways. Trend plots of percentage change in signal unit ratio are shown for (**a**) optic nerve (prechiasmatic; $P < 0.001$), (**b**) optic chiasm ($P < 0.001$), (**c**) optic tract ($P < 0.001$), and (**d**) gray matter of primary visual cortex ($P < 0.001$). Trend plots are presented with mean ± SE.

hypothesize that the observations indicate the existence of a glymphatic system in the human visual pathway

In regard to solute transport mechanisms, the original concept suggested convective flow,[4,26] and arterial pulsatile forces were also involved.[2,3] Within the interstitial spaces, diffusion also seems to be important.[27] With respect to solute transport within the human CNS, enrichment of gadobutrol over several centimeters was seen on MRI within 24 hours following intrathecally injected gadobutrol.[1,6,7] These observations correspond with the findings in the current study. Nevertheless, it was beyond the scope of the present study to thoroughly examine the mechanisms explaining the movement of CSF tracer within the visual pathway.

The findings in our study are consistent with observations in previous human studies. CSF tracer enrichment within the extravascular space of the brain parenchyma has been interpreted as supportive for the existence of a human glymphatic system.[1,7] Still, the visual pathway differ somewhat from that of the brain parenchyma in general, with the exception of the visual cortex and the retina, the visual pathway consists of white matter only in direct contact with the surrounding CSF. Axonal tracts have been proposed to

function as low resistance pathways.[28] After entrance to the interstitial space, transport of solutes along axons may therefore play an important role to mediate paravascular molecular movements within in the visual system.

Gadolinium-based contrast agents in much higher doses than used in this study may lead to serious complications.[29] Gadobutrol is a macrocyclic contrast agent, which is shown to be more stable and safe than linear agents.[30,31] Therefore, it is the recommended intravenous contrast agent for humans.[31] In a previous study, no gadobutrol was detected on MRI 4 weeks after intrathecal administration.[6]

According to previous reports,[6,7] the main entry routes of CSF tracer molecules into the human brain parenchyma are along large artery trunks at the brain surface (i.e., the anterior, middle, and posterior cerebral arteries). In the orbital segment of the optic nerve, 5 to 10 mm posterior to the eyeball, the optic nerve is pierced by the central retinal artery.[32] Analogous to the brain, this area could function as a major periarterial route facilitating the entry of gadobutrol from the subarachnoid space into the optic nerve interstitium. As the optic nerve is penetrated by multiple small branches of the dense vascular plexus of the pia mater, numerous periarterial entry routes are

likely to exist, all flushing the interstitium of the optic nerve and draining to the perivenous space. Notably, in the present study substantial gadobutrol enrichment was seen in the retrobulbar part of the optic nerve, as compared with the middle and posterior sections, corresponding to the entrance of the central retinal artery.

Another important implication of the present study is that the visual pathway can be reached through an intrathecal route. This may allow for a novel way of administering drugs to the visual system. There are no medical treatments of ophthalmic diseases approved for intrathecal administration. For systemic diseases, only a few drugs are currently approved for intrathecal administration, and this route of administration is traditionally considered to have limited therapeutic potential.[33] Although potential risks certainly exist, there could also be benefits of injecting drugs intrathecally. The BBB is bypassed, and pathology located in the extravascular space of the visual pathway may be reached more readily. In a recent paper, a brain-wide distribution of gadobutrol was seen following intrathecal injection.[6] In addition to reaching the extravascular space of the visual pathway, intrathecal administration may also allow for smaller drug doses and reduced systemic adverse effects.[34] There is also a possibility of incorporating diagnosis and treatment, so-called theranostics, via an intrathecal route, by combining diagnostic tracers and drugs (e.g., in the form of monoclonal antibodies).

In the present study, MRI did not identify any structural cause of the subjects' complaints, and they were all managed conservatively. Moreover, they had no known ophthalmic disease; thus, we consider the study subjects being close to healthy. Therefore, our study does not disclose how an impaired glymphatic function may affect the visual system. It has, however, been proposed that the glymphatic system is involved in the pathophysiology of glaucoma.[9,11,12,14,15] For instance, Wostyn et al.[15] suggested that reduced glymphatic circulation in the optic nerve may decrease clearance of toxic metabolites such as amyloid-β, which in turn might cause glaucomatous neurodegeneration. Although an intriguing hypothesis, it was beyond the scope of this work to speculate any further on how the glymphatic system might play a role in pathological processes, like for instance glaucoma. Studying the effect of a compromised glymphatic system in the visual pathway may thus provide further insight and is a relevant topic for future studies.

The subjects included in this study underwent MRI on suspicion of CSF leakage or a symptomatic pineal cyst. The MRI acquisitions were therefore not performed using a dedicated orbital MRI protocol. In some scans the visualization of the intraorbital optic nerve was restricted by image artifacts. Still, image postprocessing and manually positioning of the ROIs minimized the influence of artifacts. Another limitation of the study is the small number of study subjects. Nevertheless, the consistency of findings ameliorates issues regarding cohort size. The patients were in a supine position up to the 6- to 9-hour image time point. After that, the patient was allowed to move freely. As the tracer enrichment was consistent and within the same range for all 10 subjects, we believe a possible effect of changing postures subsequent to acquisition of the 6- to 9-hour images can be regarded as minor.

In conclusion, this study presents evidence for direct communication between CSF in the subarachnoid space and the extravascular space of the human visual pathway. We suggest this finding may indicate the presence of a glymphatic system involving visual pathway in humans. Evidence of a visual pathway glymphatic system could represent a paradigm shift in understanding the pathophysiology of various ocular diseases and provide for new diagnostic and therapeutic approaches. Further studies are needed to explore the present findings' role in the visual pathway.

References

1. Eide PK, Vatnehol SAS, Emblem KE, Ringstad G. Magnetic resonance imaging provides evidence of glymphatic drainage from human brain to cervical lymph nodes. *Sci Rep*. 2018;8: 7194.

2. Iliff JJ, Wang M, Zeppenfeld DM, et al. Cerebral arterial pulsation drives paravascular CSF-interstitial fluid exchange in the murine brain. *J Neurosci*. 2013;33:18190–18199.

3. Rasmussen MK, Mestre H, Nedergaard M. The glymphatic pathway in neurological disorders. *Lancet Neurol*. 2018;17: 1016–1024.

4. Iliff JJ, Wang M, Liao Y, et al. A paravascular pathway facilitates CSF flow through the brain parenchyma and the clearance of interstitial solutes, including amyloid beta. *Sci Transl Med*. 2012; 4:147ra111.

5. Plog BA, Nedergaard M. The glymphatic system in central nervous system health and disease: past, present, and future. *Annu Rev Pathol*. 2018;13:379–394.

6. Ringstad G, Valnes LM, Dale AM, et al. Brain-wide glymphatic enhancement and clearance in humans assessed with MRI. *JCI Insight*. 2018;3:121537.

7. Ringstad G, Vatnehol SAS, Eide PK. Glymphatic MRI in idiopathic normal pressure hydrocephalus. *Brain*. 2017;140: 2691–2705.

8. Denniston AK, Keane PA, Aojula A, Sinclair AJ, Mollan SP. The ocular glymphatic system and idiopathic intracranial hypertension: author response to hypodense holes and the ocular glymphatic system. *Invest Ophthalmol Vis Sci*. 2017;58:1134– 1136.

9. Wostyn P, De Groot V, Van Dam D, Audenaert K, De Deyn PP, Killer HE. The glymphatic system: a new player in ocular diseases? *Invest Ophthalmol Vis Sci*. 2016;57:5426–5427.

10. Denniston AK, Keane PA. Paravascular pathways in the eye: is there an 'ocular glymphatic system'? *Invest Ophthalmol Vis Sci*. 2015;56:3955–3956.

11. Wostyn P, De Groot V, Van Dam D, Audenaert K, Killer HE, De Deyn PP. The glymphatic hypothesis of glaucoma: a unifying concept incorporating vascular, biomechanical, and biochemical aspects of the disease. *Biomed Res Int*. 2017;2017: 5123148.

12. Wostyn P, Killer HE, De Deyn PP. Glymphatic stasis at the site of the lamina cribrosa as a potential mechanism underlying

open-angle glaucoma. *Clin Exp Ophthalmol*. 2017;45:539–547.

13. Mathieu E, Gupta N, Ahari A, Zhou X, Hanna J, Yucel YH. Evidence for cerebrospinal fluid entry into the optic nerve via a glymphatic pathway. *Invest Ophthalmol Vis Sci* 2017;58:4784–4791.

14. Mathieu E, Gupta N, Paczka-Giorgi LA, et al. Reduced cerebrospinal fluid inflow to the optic nerve in glaucoma. *Invest Ophthalmol Vis Sci*. 2018;59:5876–5884.

15. Wostyn P, Van Dam D, Audenaert K, Killer HE, De Deyn PP, De Groot V. A new glaucoma hypothesis: a role of glymphatic system dysfunction. *Fluids Barriers CNS*. 2015;12:16.

16. Kress BT, Iliff JJ, Xia M, et al. Impairment of paravascular clearance pathways in the aging brain. *Ann Neurol*. 2014;76:845–861.

17. Xie L, Kang H, Xu Q, et al. Sleep drives metabolite clearance from the adult brain. *Science*. 2013;342:373–377.

18. Eide PK, Ringstad G. MRI with intrathecal MRI gadolinium contrast medium administration: a possible method to assess glymphatic function in human brain. *Acta Radiol Open*. 2015;4:2058460115609635.

19. Asgari M, de Zelicourt D, Kurtcuoglu V. How astrocyte networks may contribute to cerebral metabolite clearance. *Sci Rep*. 2015;5:15024.

20. Ho JD, Yeh R, Sandstrom A, et al. Crystal structure of human aquaporin 4 at 1.8 A and its mechanism of conductance. *Proc Natl Acad Sci U S A*. 2009;106:7437–7442.

21. Eide PK, Hansson HA. Astrogliosis and impaired aquaporin-4 and dystrophin systems in idiopathic normal pressure hydrocephalus. *Neuropathol Appl Neurobiol*. 2018;44:474–490.

22. Hasan-Olive MM, Enger R, Hansson HA, Nagelhus EA, Eide PK. Loss of perivascular aquaporin-4 in idiopathic normal pressure hydrocephalus. *Glia*. 2019;67:91–100.

23. Cheng KT. Gadobutrol. In: *Molecular Imaging and Contrast Agent Database (MICAD)*. Bethesda: National Center for Biotechnology Information; 2004:2–8.

24. Nicholson C, Tao L. Hindered diffusion of high molecular weight compounds in brain extracellular microenvironment measured with integrative optical imaging. *Biophys J*. 1993;65:2277–2290.

25. Iliff JJ, Lee H, Yu M, et al. Brain-wide pathway for waste clearance captured by contrast-enhanced MRI. *J Clin Invest*. 2013;123:1299–1309.

26. Jessen NA, Munk AS, Lundgaard I, Nedergaard M. The glymphatic system: a beginner's guide. *Neurochem Res*. 2015;40:2583–2599.

27. Holter KE, Kehlet B, Devor A, et al. Interstitial solute transport in 3D reconstructed neuropil occurs by diffusion rather than bulk flow. *Proc Natl Acad Sci U S A*. 2017;114:9894–9899.

28. Abbott NJ. Evidence for bulk flow of brain interstitial fluid: significance for physiology and pathology. *Neurochem Int*. 2004;45:545–552.

29. Park KW, Im SB, Kim BT, Hwang SC, Park JS, Shin WH. Neurotoxic manifestations of an overdose intrathecal injection of gadopentetate dimeglumine. *J Korean Med Sci*. 2010;25:505–508.

30. Robert P, Violas X, Grand S, et al. Linear gadolinium-based contrast agents are associated with brain gadolinium retention in healthy rats. *Invest Radiol*. 2016;51:73–82.

31. Malayeri AA, Brooks KM, Bryant LH, et al. National Institutes of Health perspective on reports of gadolinium deposition in the brain. *J Am Coll Radiol*. 2016;13:237–241.

32. Singh S, Dass R. The central artery of the retina. I. Origin and course. *Br J Ophthalmol*. 1960;44:193–212.

33. Pardridge WM. The blood-brain barrier: bottleneck in brain drug development. *NeuroRx*. 2005;2:3–14.

34. Bottros MM, Christo PJ. Current perspectives on intrathecal drug delivery. *J Pain Res*. 2014;7:615–626.